

Mechanical, Thermal and Morphological Properties of Injection Molded Poly(lactic acid)/Calcium Carbonate Nanocomposites

Wen Shyang Chow^{1*}, Ying Ying Leu¹, Zainal Arifin Mohd Ishak¹

Received 09 June 2015; accepted after revision 29 September 2015

Abstract

In this work, mechanical and thermal properties of maleated ethylene-propylene rubber (EPR-g-MAH) toughened poly(lactic acid) (PLA)/nano-precipitated calcium carbonate (NPCC) nanocomposites were investigated. It was found that elongation at break of PLA/NPCC was increased with increasing EPR-g-MAH content up to 15 phr (parts per hundred resin). The investigations on the crystallization behaviours demonstrated that the NPCC acted as nucleating agent for the PLA. However, the degree of crystallinity of PLA was reduced by the addition of EPR-g-MAH which appears to be due to encapsulation of NPCC by the maleated rubber. Dispersion of NPCC was observed using transmission electron microscopy (TEM), and it was revealed that both nano-dispersed and agglomerates NPCC exist in the PLA matrix. Moreover, encapsulation of NPCC was favored in the presence of EPR-g-MAH.

Keywords

nanocomposites, poly(lactic acid), nano-calcium carbonate, maleated rubber, properties

1 Introduction

In recent years, the interest in renewable and biodegradable polymeric materials has increased enormously in the academic and industry community. Poly(lactic acid) (PLA) produced from renewable resources has become attractive and popular in various fields, such as packaging, textile and automotives industries. Among all biodegradable polymers, PLA is a very promising eco-friendly alternative compared to traditional petroleum based thermoplastics. This is attributed to its high modulus and strength, biodegradability, and superior transparency. Among the limitation of PLA, its low thermal stability and brittleness has to be mentioned [1-4].

Several approaches have been used to improve the properties of PLA, for example, incorporation of filler and additives, blending with flexible polymers, and adding of functionalized rubber and tougheners. Recently, PLA-based nanocomposites prepared by the incorporation of nanofillers (e.g. nanoclay, nano-calcium carbonate, titanium oxide nanoparticles, cellulose nanofiber and carbon nanotube) exhibited remarkable improvement in mechanical and thermal properties, dimensional stability, barrier and physicochemical behaviours [5-10].

Although the hybridization of polymer and nanoparticle can be a potential class of materials, there are few issues always need to be considered, e.g. compatibility between polymer and nanoparticles, dispersion and distribution of nanoparticles, brittleness and toughness of the polymer nanocomposites, as well as their ease of processing. Therefore, chemical and physical modifications are often applied to achieve these objectives. Similarly, the need of toughness and impact strength improvement of PLA/nanofiller nanocomposites was recognized and most of the related works are based on chemical and physical modification. There is a need to improve the toughness and flexibility of PLA so that it can compete with commodity thermoplastics. Thus, various approaches including copolymerization, plasticization, and blending with elastomeric materials have been carried out to enhance the impact properties and toughness of PLA.

Maleated rubbers such as maleic anhydride grafted ethylene-propylene rubber (EPR-g-MAH) and maleic anhydride grafted styrene-ethylene/butylene-styrene copolymers

¹ School of Materials and Mineral Resources Engineering, Engineering Campus, Universiti Sains Malaysia, Nibong Tebal 14300 Penang, Malaysia

* Corresponding author, e-mail: shyang@usm.my

(SEBS-g-MAH), has been used as polymeric compatibilizer, interfacial modifier and toughening agent. Recent reports have proved that the addition of EPR-g-MAH could enhance the dispersion of the nanoclay and improve the mechanical and thermal properties of various polymer nanocomposites, including polyamide 6/polypropylene/organoclay nanocomposites [11], PLA/clay nanocomposites [12-14].

In our previous work we have examined the impact strength, elongation at break and thermal stability of PLA/organo-montmorillonite and PLA/nano-precipitated calcium carbonate nanocomposites, and found that their properties improved significantly by the addition of SEBS-g-MAH [15,16]. The aim of this work is to improve the flexibility and thermal properties of the PLA/NPCC by the addition of EPR-g-MAH. Accordingly, the mechanical, thermal and morphological properties of PLA/NPCC/EPR-g-MAH are discussed thoroughly in this paper.

2 Experimental

2.1 Materials

PLA (Ingeo™ 3051D) was supplied by NatureWorks LLC®, USA. The specific gravity and melt flow index of the PLA are 1.25 and 25 g/10 min (2.16 kg load, 210°C), respectively. The stearic acid treated NPCC (Zancarb CC-R; particle size: 40–80 nm; specific gravity: 2.50) was supplied by Zantat Sdn. Bhd (Kuala Lumpur, Malaysia). EPR-g-MAH was purchased from Shanghai Jianqiao Plastic Co. Ltd., China. The melt flow index and specific gravity of the EPR-g-MAH were 0.2 g/10 min (2.16 kg loads, 230°C) and 0.88 respectively. The grafting content of MAH on EPR is approximately 1.0 wt%. The ethylene/propylene ratio of the material was 70/30 (wt/wt). The designation and composition for PLA/NPCC nanocomposites are shown in Table 1.

2.2 Preparation of PLA/NPCC nanocomposites

All the ingredients (e.g. PLA pellets, NPCC powders, and EPR-g-MAH pellets) were dried at 80°C for 15 hours in vacuum oven (Memmert GmbH, model: VO500, Germany) prior to extrusion. Then, the ingredients were pre-mixed by tumbling process. The melt-compounding was performed using a co-rotating twin-screw extruder (Sino-Alloy Machinery, model: PSM30, Taiwan). The temperature zone and screw speed were set in the range of 160–190°C and 150 rpm, respectively. The PLA nanocomposites specimen [tensile (ASTM D638 type I); flexural (ASTM D790)] was injection moulded using an injection moulding machine (Haitian, model: HTF86X1, China). The barrel temperatures were set at a range of 165–190°C, from the feeding section to the nozzle, respectively. Prior to injection moulding process, the PLA extrudates were dried in a vacuum oven at 80°C for 15 hours.

Table 1 Material designation and composition for PLA/NPCC/EPR-g-MAH nanocomposites.

Materials designation	Composition		
	PLA (wt%)	NPCC (wt%)	EPR-g-MAH (phr)
PLA	100	-	-
PLA/NPCC	98	2	-
PLA/NPCC/EPR-g-MAH 5	98	2	5
PLA/NPCC/EPR-g-MAH 10	98	2	10
PLA/NPCC/EPR-g-MAH 15	98	2	15
PLA/NPCC/EPR-g-MAH 20	98	2	20

2.3 Characterization of PLA/NPCC nanocomposites

2.3.1 Morphology assessment

TEM measurements were carried out with an energy filtering transmission electron microscope (Carl Zeiss, model: Zeiss Libra 120 Plus, USA) operating at an accelerating voltage of 120 kV. The specimens were prepared using an ultramicrotome (Boeckeler Instruments, model: PT-PC PowerTome, USA). Ultra-thin sections of about 50 nm in thickness of the PLA nanocomposite specimen was cut with a diamond knife (Diatome, model: ultra 45°, Switzerland) at room temperature. Then the specimen was stained with osmium tetroxide (OsO₄) for 1 h.

2.3.2 Mechanical tests

Tensile tests were performed according to the ASTM D 638 using a universal testing machine (Instron, model: Instron 3366, USA). The tensile tests were conducted at a crosshead speed of 5 mm/min. Tensile modulus, strength and elongation at break of the composites was determined. Flexural tests were carried out according to the ASTM D790 using a universal testing machine (Instron, model: Instron 3366, USA). The flexural tests were done under three-point bending configuration at crosshead speed of 1.5 mm/min and support span length of 56 mm (16 x 3.5 mm). Five specimens from each formulation were tested. Flexural strength and flexural modulus were determined.

2.3.3 Thermal tests

The thermal decomposition temperature of the PLA nanocomposites was characterized using a thermogravimetric analyzer (Perkin Elmer, model: Pyris 6, USA). The specimens were heated from room temperature to 600°C at a heating rate of 10°C/min in nitrogen atmosphere.

Differential scanning calorimeter (Perkin Elmer, model: DSC 6, USA) was used to evaluate the thermal behaviour of the PLA nanocomposite specimens. The specimens were scanned from 30°C to 190°C at a heating rate of 10°C/min and held for

1 minute at 190°C. Then, they were cooled from 190°C to 30°C at a cooling rate of 10°C/min and held for 1 minute at 30°C. The glass transition temperature (T_g), melting temperature (T_m), cold-crystallization temperature (T_{cc}), and degree of crystallinity (χ_c) were determined. The heat of fusion of 100% crystalline PLA (ΔH_f) is approximately 93.6 J/g [17].

3 Results and Discussion

3.1 Transmission electron microscopy (TEM)

Figure 1 shows the TEM images of PLA/NPCC nanocomposites. It can be seen that the NPCC nanoparticles are in cubic shape with dimension of 40–80 nm. Both nano-dispersed NPCC and agglomerates of NPCC can be observed in the PLA matrix. Agglomerations of NPCC can be attributed to high surface energy of the particles. Figure 2 and 3 shows the TEM images of PLA/NPCC nanocomposites consisting of 5 and 20 phr of EPR-g-MAH respectively. In Figure 2 and 3, the dark grey region (i.e. region that stained by osmium tetroxide) with dimension of approximately 1–2 μm can be ascribed to the EPR-g-MAH. Similar observation can be found on SEBS-g-MAH toughened PLA/NPCC nanocomposites, as reported in our previous work [16]. From Figure 2, one may notice that a few of NPCC nanoparticles are embedded in EPR-g-MAH. On the other hand, a higher number of NPCC were encapsulated by the maleated rubber in the PLA/NPCC/EPR-g-MAH20 (c.f. Fig. 3). This can be associated to the affinity between NPCC and EPR-g-MAH.

3.2 Mechanical properties of PLA nanocomposites

Table 2 shows the mechanical properties of neat PLA and its nanocomposites. As expected, the tensile modulus of PLA/ NPCC nanocomposites reduced marginally with the increasing content of EPR-g-MAH. Note that the tensile strength of PLA/NPCC nanocomposites also decreased with the increasing loading of EPR-g-MAH. This is associated with the lower modulus and elastomeric nature of the EPR-g-MAH.

The elongation at break of PLA/NPCC nanocomposite increased up to 148% by the incorporation of 20 phr of EPR-g-MAH. The improvement in ductility of the PLA nanocomposites can be attributed to the elastomeric behaviour of the maleated rubbers which could contribute to the enhancement of toughness. Under the applied tensile stress, the maleated rubbers could absorb the fracture energy and prevent the propagation of the crack front which subsequently could lead to an increase in ductility of the nanocomposites. Moreover, the encapsulation of the NPCC particles by the EPR-g-MAH (as observed in the TEM, see Fig. 2 and 3) may avoid highly localized stress concentrations which could facilitate the PLA samples to elongate to a greater extent. It can be noted that the presence of EPR-g-MAH decreased the flexural modulus and strength of the PLA/NPCC nanocomposites. The effect became prominent as the loadings of EPR-g-MAH increased. This trend resembles to that of the tensile properties.

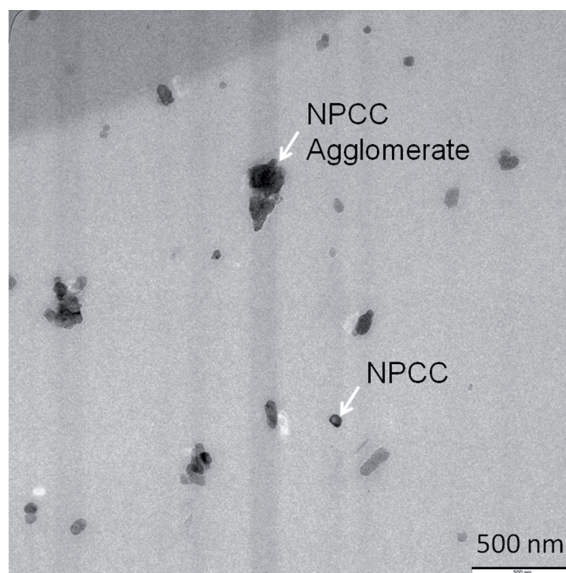


Fig. 1 TEM image of PLA/NPCC nanocomposite.

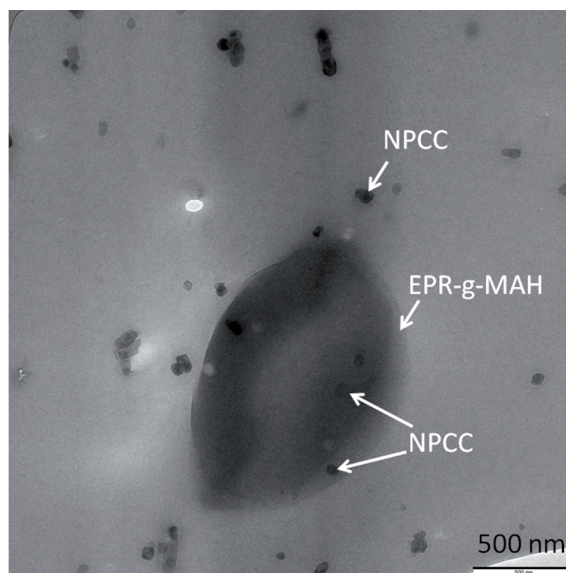


Fig. 2 TEM image of PLA/NPCC/EPR-g-MAH-5 nanocomposite.

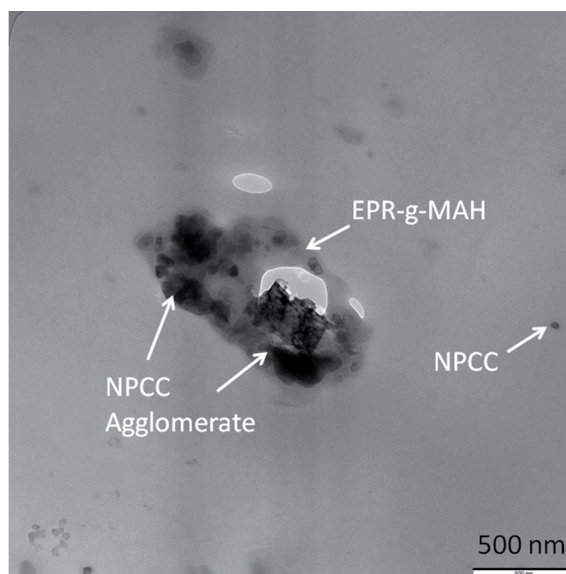


Fig. 3 TEM image of PLA/NPCC/EPR-g-MAH-20 nanocomposite.

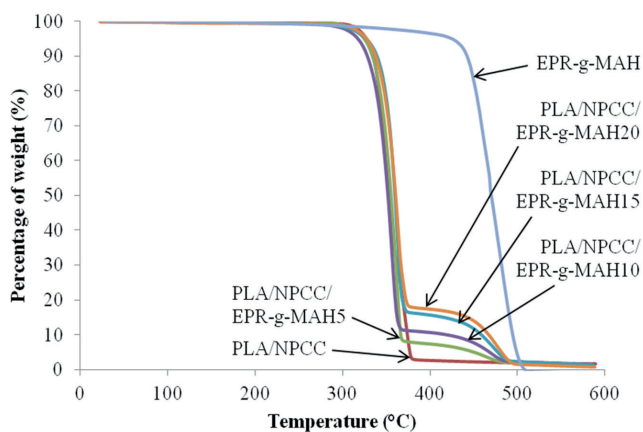
Table 2 Mechanical properties of PLA/NPCC/EPR-g-MAH nanocomposites.

Materials designation	TS (MPa)	EB (%)	TM (GPa)	FS (MPa)	FM (GPa)
PLA	59.4 ± 0.43	8.4 ± 0.16	1.18 ± 0.02	97.0 ± 0.2	3.61 ± 0.07
PLA/NPCC	58.7 ± 1.26	12.4 ± 1.18	1.23 ± 0.03	96.1 ± 1.5	3.79 ± 0.07
PLA/NPCC/ EPR-g-MAH 5	34.7 ± 2.25	29.4 ± 1.74	1.02 ± 0.02	78.2 ± 2.5	3.53 ± 0.08
PLA/NPCC/ EPR-g-MAH 10	30.4 ± 1.85	31.2 ± 1.05	0.97 ± 0.01	67.6 ± 1.1	3.20 ± 0.06
PLA/NPCC/ EPR-g-MAH 15	29.1 ± 0.55	31.7 ± 2.25	0.90 ± 0.02	60.8 ± 0.9	2.83 ± 0.02
PLA/NPCC/ EPR-g-MAH 20	23.3 ± 1.58	30.8 ± 0.83	0.83 ± 0.02	54.1 ± 1.6	2.48 ± 0.10

(Note: TS = tensile strength; EB = elongation at break; TM = tensile modulus; FS = flexural strength; FM = flexural modulus).

3.3 Thermal properties of PLA nanocomposites

The thermal stabilities of PLA/NPCC composites were evaluated by TGA with a temperature range from room temperature to 600°C. Figure 4 shows the TGA curves for PLA/NPCC and PLA/NPCC/EPR-g-MAH nanocomposites. The decomposition temperature is summarized in Table 3. The T_5 corresponding to the temperature at 5% weight loss. The decomposition temperature in the range of 335–362°C is related to the thermal decomposition of the PLA. The decomposition temperature of NPCC starts at 250°C and the char residue is approximately 96.9% at the temperature of 600°C. The mass loss of NPCC is attributed to the decomposition of stearic acid surface modifier [16]. It is also found that the decomposition of organic modifier may accelerate thermal decomposition for the PLA/NPCC composites. It can be seen that the first onset decomposition temperatures (T_{d1}) of PLA/NPCC nanocomposites shifted to higher temperature by the addition of EPR-g-MAH. This can be due to the higher thermal stability of EPR-g-MAH.

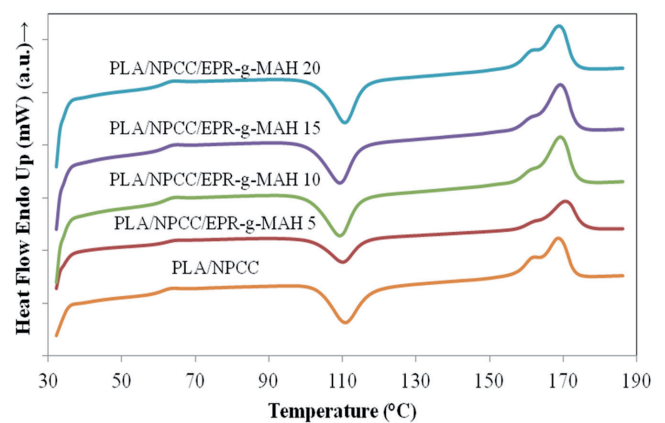
**Fig. 4** TGA curves of PLA/NPCC/EPR-g-MAH nanocomposites.**Table 3** TGA data of PLA/NPCC/EPR-g-MAH nanocomposites.

Materials designation	Decomposition temperature (°C)		
	T_{d1}	T_{d2}	T_5
PLA	353.4	-	346.0
PLA/NPCC	334.6	-	327.2
EPR-g-MAH	448.2	-	426.9
PLA/NPCC/EPR-g-MAH 5	343.4	435.7	324.3
PLA/NPCC/EPR-g-MAH 10	339.4	440.5	317.8
PLA/NPCC/EPR-g-MAH 15	348.1	441.3	327.0
PLA/NPCC/EPR-g-MAH 20	346.2	447.7	327.3

(Note: T_{d1} = first onset decomposition temperature; T_{d2} = second onset decomposition temperature; T_5 = temperature at 5% weight loss).

Figure 5 shows the DSC curves of PLA/NPCC nanocomposites. The DSC thermal characteristics (e.g. T_g , T_{cc} , T_m) of the PLA nanocomposites are summarized in Table 4. The glass transition temperatures (T_g) of the PLA and its nanocomposites remained unchanged. PLA shows a melting temperature peak (T_{m1}) at 168.8°C with a small shoulder peak (T_{m2}) at 161.2°C. Bimodal melting peaks are observed in all PLA/NPCC composites with and without EPR-g-MAH. It is well known that multiple melting behaviour of PLA is depends on crystallization conditions (thermal prehistory), melt-recrystallization and T_c value [18-20]. Double melting endotherms are commonly found in PLA which crystallized at T_c in the temperature range of 110–130°C [21]. In this study, the PLA/NPCC/EPR-g-MAH nanocomposites recorded T_c approximately 110°C, thus this crystallization temperature may favour the formation of double-peak melting endotherms.

From Table 4, it can be seen that the degree of crystallinity of PLA/NPCC nanocomposite is slightly higher than the neat PLA. The addition of NPCC particles may lead to the formation of more nucleation sites for the crystallization of PLA. It is known that different structures and surface characteristics of nanofillers could influence the crystallization of a polymer matrix [22].

**Fig. 5** DSC curves of PLA/NPCC/EPR-g-MAH nanocomposites.

The presence of calcium carbonate greatly affected the crystallization of the polymer by acting as multi-nuclei, leading to more spherulites formation [23]. On the contrary, the incorporation of EPR-g-MAH reduces the degree of crystallinity of PLA/NPCC nanocomposites. This is attributed to the encapsulation of NPCC by EPR-g-MAH, which may diminish the efficiency of NPCC as nucleating agent in the crystallization of PLA.

Table 4 DSC thermal characteristics of PLA/NPCC/EPR-g-MAH nanocomposites.

Materials designation	T_g (°C)	T_{cc} (°C)	T_{m1} (°C)	T_{m2} (°C)	χ_c (%)
PLA	60.9	112.7	168.8	161.2	33.3
PLA/NPCC	60.6	110.8	168.6	160.1	38.0
PLA/NPCC/EPR-g-MAH 5	61.9	110.0	170.4	161.2	29.7
PLA/NPCC/EPR-g-MAH 10	61.7	109.5	169.6	161.1	33.0
PLA/NPCC/EPR-g-MAH 15	61.7	109.3	169.2	161.2	36.0
PLA/NPCC/EPR-g-MAH 20	61.0	110.6	168.9	161.3	34.0

4 Conclusions

The PLA/NPCC/EPR-g-MAH nanocomposites were prepared through a twin screw extruder followed by injection molding. EPR-g-MAH increased elongation at break but at the cost of modulus and strength for the PLA/NPCC nanocomposites. From the DSC results, it was found that NPCC acted as nucleating agent for PLA. However, EPR-g-MAH reduced degree of crystallinity of PLA/NPCC which can be due to the encapsulation of NPCC by EPR-g-MAH. The thermal stability of PLA/NPCC was improved slightly with the addition of EPR-g-MAH. The dispersion of NPCC was affected by EPR-g-MAH content, as can be shown from the TEM results that encapsulation of NPCC and nano-particle agglomerates tends to occur in the presence of high loading of the maleated rubber.

Acknowledgments

This study was funded by the Universiti Sains Malaysia Research University (RU) Grant [contract grant number: 814199] and USM Postgraduate Research Grant Scheme [contract grant number: USM-RU-PGRS 8033002].

References

[1] Raquez, J. M., Habibi, Y., Murariu, M., Dubois, P. "Polylactide (PLA)-based nanocomposites." *Progress in Polymer Science*. 38 (10-11). pp. 1504-1542. 2013. DOI: [10.1016/j.progpolymsci.2013.05.014](https://doi.org/10.1016/j.progpolymsci.2013.05.014)

[2] Ray, S. S., Okamoto, M. "Biodegradable polylactide and its nanocomposites: Opening a new dimension for plastics and composites." *Macromolecular Rapid Communication*. 24 (14). pp. 815-840. 2003. DOI: [10.1002/marc.200300008](https://doi.org/10.1002/marc.200300008)

[3] Garlotta, D. "A Literature review of poly(lactic acid)." *Journal of Polymers and the Environment*. 9 (2). pp. 63-84. 2002. DOI: [10.1023/A:1020200822435](https://doi.org/10.1023/A:1020200822435)

[4] Bocz, K., Domonkos, M., Igricz, T., Kmetty, A., Bárány, T., Marosi, G. "Flame retarded self-reinforced poly(lactic acid) composites of outstanding impact resistance." *Composites: Part A*. 70. pp. 27-34. 2015. DOI: [10.1016/j.compositesa.2014.12.005](https://doi.org/10.1016/j.compositesa.2014.12.005)

[5] Zhou, Q., Xanthos, M. "Nanosize and microsize clay effects on the kinetics of the thermal degradation of poly(lactides)." *Polymer Degradation and Stability*. 94 (3). pp. 327-338. 2009. DOI: [10.1016/j.polyimdegradstab.2008.12.009](https://doi.org/10.1016/j.polyimdegradstab.2008.12.009)

[6] Pavlidou, S., Papaspyrides, C.D. "A review on polymer-layered silicate nanocomposites." *Progress in Polymer Science*. 33 (12). pp. 1119-1198. 2008. DOI: [10.1016/j.progpolymsci.2008.07.008](https://doi.org/10.1016/j.progpolymsci.2008.07.008)

[7] Long, J., Zhang, J. W., Wolcott, M. P. "Comparison of polylactide/nanosized calcium carbonate and polylactide/montmorillonite composites: Reinforcing effects and toughening mechanisms." *Polymer*. 48 (26). pp. 7632-7644. 2007. DOI: [10.1016/j.polymer.2007.11.001](https://doi.org/10.1016/j.polymer.2007.11.001)

[8] Chen, C., Gang, L.V., Pan, C., Song, M., Wu, C. H., Guo, D., Wang, X.M., Chen, B., Gu. Z. "Poly(lactic acid) (PLA) based nanocomposites-a novel way of drug releasing." *Biomedical Materials*. 2 (4). pp. L1-L4. 2007. DOI: [10.1088/1748-6041/2/4/L01](https://doi.org/10.1088/1748-6041/2/4/L01)

[9] Iwatake, A., Nogi, M., Yano, H. "Cellulose nanofiber-reinforced polylactic acid." *Composites Science and Technology*. 68 (9). pp. 2103-2106. 2008. DOI: [10.1016/j.compscitech.2008.03.006](https://doi.org/10.1016/j.compscitech.2008.03.006)

[10] Hapuarachchi, T. D., Peijs, T. "Multiwalled carbon nanotubes and sepiolite nanoclays as flame retardants for polylactide and its natural fibre reinforced composites." *Composites Part A: Applied Science and Manufacturing*. 41 (8). pp. 954-963. 2010. DOI: [10.1016/j.compositesa.2010.03.004](https://doi.org/10.1016/j.compositesa.2010.03.004)

[11] Chow, W. S., Bakar, A. A., Mohd Ishak, Z. A., Karger-Kocsis, J., Ishiaku, U. S. "Effect of maleic anhydride-grafted ethylene-propylene rubber on the mechanical, rheological and morphological properties of organoclay reinforced polyamide 6/polypropylene nanocomposites." *European Polymer Journal*. 41 (4). pp. 687-696. 2005. DOI: [10.1016/j.eurpolymj.2004.10.041](https://doi.org/10.1016/j.eurpolymj.2004.10.041)

[12] Chow, W. S., Lok, S. K. "Effect of EPM-g-MAH on the flexural and morphological properties of poly(lactic acid)/organo-montmorillonite nanocomposites." *Journal of Thermoplastic Composite Materials*. 21 (3). pp. 265-277. 2008. DOI: [10.1177/0892705708089477](https://doi.org/10.1177/0892705708089477)

[13] Chow, W. S., Lok, S. K. "Thermal properties of poly(lactic acid)/organo-montmorillonite nanocomposites." *Journal of Thermal Analysis and Calorimetry*. 95 (2). pp. 627-632. 2009. DOI: [10.1007/s10973-007-8975-x](https://doi.org/10.1007/s10973-007-8975-x)

[14] Chow, W. S., Leu, Y. Y., Mohd Ishak, Z. A. "Poly(lactic acid) nanocomposites with improved impact and thermal properties." *Journal of Composite Materials*. 48 (2). pp. 155-163. 2014. DOI: [10.1177/0021998312469891](https://doi.org/10.1177/0021998312469891)

[15] Leu, Y. Y., Mohd Ishak, Z. A., Chow, W. S. "Mechanical, thermal, and morphological properties of injection molded poly(lactic acid)/SEBS-g-MAH/organo-montmorillonite nanocomposites." *Journal of Applied Polymer Science*. 124 (2). pp. 1200-1207. 2012. DOI: [10.1002/app.35084](https://doi.org/10.1002/app.35084)

[16] Chow, W. S., Leu, Y. Y., Mohd Ishak, Z. A. "Effects of SEBS-g-MAH on the properties of injection moulded poly(lactic acid)/nano-calcium carbonate composites." *Express Polymer Letters*. 6 (6). pp. 503-510. 2012. DOI: [10.3144/expresspolymlett.2012.53](https://doi.org/10.3144/expresspolymlett.2012.53)

[17] Wang, H., Sun, X., Seib, P. "Strengthening blends of poly(lactic acid) and starch with methylenediphenyl diisocyanate." *Journal of Applied Polymer Science*. 82 (7). pp. 1761-1767. 2001. DOI: [10.1002/app.2018](https://doi.org/10.1002/app.2018)

[18] Di Lorenzo, M. L. "Calorimetric analysis of the multiple melting behavior of poly(L-lactic acid)." *Journal of Applied Polymer Science*. 100 (4). pp. 3145-3151. 2006. DOI: [10.1002/app.23136](https://doi.org/10.1002/app.23136)

- [19] Calafel, M. I., Remiro, P. M., Cortázar, M. M., Calahorra, M. E. "Cold crystallization and multiple melting behavior of poly(l-lactide) in homogeneous and in multiphasic epoxy blends." *Colloid & Polymer Science*. 288 (3). pp. 283-296. 2010. DOI: [10.1007/s00396-009-2156-3](https://doi.org/10.1007/s00396-009-2156-3)
- [20] Sarasua, J. R., Rodríguez, N. L., Arraiza, A. L., Meaurio E. "Stereoselective crystallization and specific interactions in polylactides." *Macromolecules*. 38 (20). pp. 8362-8371. 2005. DOI: [10.1021/ma051266z](https://doi.org/10.1021/ma051266z)
- [21] Pan, P., Inoue, Y. "Polymorphism and isomorphism in biodegradable polyesters." *Progress in Polymer Science*. 34 (7). pp. 605-640. 2009. DOI: [10.1016/j.progpolymsci.2009.01.003](https://doi.org/10.1016/j.progpolymsci.2009.01.003)
- [22] Sun, L., Yang, J. T., Lin, G. Y., Zhong, M. Q. "Crystallization and thermal properties of polyamide 6 composites filled with different nanofillers." *Materials Letters*. 61 (18). pp. 3963-3966. 2007. DOI: [10.1016/j.matlet.2006.12.090](https://doi.org/10.1016/j.matlet.2006.12.090)
- [23] Zhang, Q. X., Yu, Z. Z., Xie, X. L., Mai, Y. W. "Crystallization and impact energy of polypropylene/CaCO₃ nanocomposites with nonionic modifier." *Polymer*. 45 (17). pp. 5985-5994. 2004. DOI: [10.1016/j.polymer.2004.06.044](https://doi.org/10.1016/j.polymer.2004.06.044)